Liquid helium, vortices, helices and laser light scattering

1999 J. Phys.: Condens. Matter 11 7711

(http://iopscience.iop.org/0953-8984/11/40/304)

J. Phys.: Condens. Matter **11** (1999) 7711–7722. Printed in the UK PII: S0953-8984(99)03152-5

Liquid helium, vortices, helices and laser light scattering

J M Vaughan

Defence Evaluation and Research Agency, St Andrews Road, Malvern, Worcestershire WR14 3PS, UK

Received 1 April 1999

Abstract. Initial consideration of quantized vortices led to a detailed study of light scattering in liquid helium with very high resolution classical instruments and observation of novel spectra. The need for yet higher resolution led in turn to study of time-domain spectroscopy. Precise control of optical wave front and coherence is required in these techniques, and this initiated the discovery of optical vortices with multistart helical cophasal surfaces as demonstrated by unusual interference fringes. Finally the application of such laser scattering techniques has revealed the presence of descending ring vortices in thunderstorm microbursts and has been used to study the powerful wake vortices generated by aircraft.

1. Introduction

Circular or rotational flow has long been a subject of fascination—stretching back at least to Leonardo's remarkable drawings of turbulence and his studies for easing the rapids in the River Arno. In the present short paper this topic offers a unifying theme to snapshots of laser work in which I have been involved stretching back over 30 years to Birmingham. Starting with vortices in liquid helium this progresses through light scattering in liquid helium, optical multistart helices, descending ring vortices in the atmosphere and the powerful wake vortices generated by aircraft.

2. Light scattering from liquid helium

I came to Birmingham University, after two years in the United States, to work with Professor Joe Vinen in autumn 1968. Our original intention had been to study quantized rotating vortices in superfluid helium which Joe had so notably discovered a few years before. At Princeton University I had in fact been attempting to investigate whether such vortices assumed a regular spatial array, analogous to the effects observed in superconductors. This rather fanciful experiment had involved placing small moveable particles on the lower surface of a rotating cell of liquid helium, illuminating these with a collimated laser beam, and examining the scattered light for any diffraction pattern that would reveal order or symmetry. The hope was that quantized vortices would latch on to the particles and after a period of steady rotation some regularity in the pattern would become established. At Birmingham after a few months of reading and discussion it was evident that light scattering from liquid helium was itself a very interesting topic and possibly feasible. It would also combine my own optical and spectroscopic expertise and the existing low temperature capabilities and facilities of Joe's low temperature group. Additionally at the time there was a strong link with the Physics

0953-8984/99/407711+12$30.00

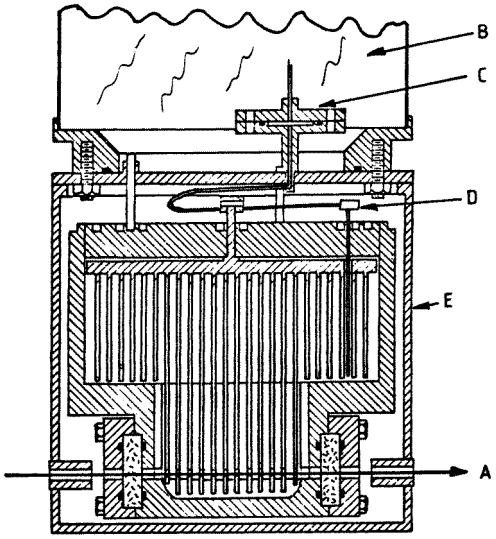

Figure 1. A scattering cell developed by Vaughan and Vinen for the study of liquid helium. The windows were sealed with indium 'O' rings and the body and internal fins were made of high conductivity copper, to promote temperature uniformity close to the λ-point. A: laser beam; B: main liquid helium bath; C: millipore filter; D: cell filling line; E: liquid helium cooled shield around cell.

Group at the Royal Radar Establishment (now DERA), Malvern, about 30 miles away; in particular Dr Roy Pike had a high resolution Fabry–Perot spectrometer that might be adapted. Thus in early 1969 we set up a collaborative program to study light scattering from liquid helium in its different forms.

The task offered formidable difficulties, both spectroscopic and cryogenic. With its low density and temperature the light scattering from liquid helium was extremely weak and would be unlikely to exceed a few photon counts per second. In addition the spectral resolution had to be extremely high—ideally down to a few MHz—and this was far in advance of anything previously demonstrated with classical Fabry–Perot spectrometry. Cryogenically there was the problem of introducing up to 300 mW in a focused laser beam, collecting the weak scattered light, and at the same time maintaining the liquid helium at precisely controllable temperatures above and below the superfluid λ-point transition. Our initial designs were based on a simple 90° light scattering cell drilled in a cruciform shape out of a copper block with four high quality fused silica windows, set at the base of a ^{4}He cryostat. The windows were simply sealed with compressed indium wire, as I had employed at Princeton, and were remarkably effective even against leaks of superfluid helium—somewhat I suspect to Joe's surprise. A later, considerably more sophisticated, high pressure, scattering cell is shown in figure 1.

The detailed theories of light scattering are complex but the basic phenomena, certainly for liquid helium, have an immediate physical elegance and simplicity. Light is scattered from refractive index fluctuations which arise from density fluctuations. Such density fluctuations can be decomposed into pressure fluctuations and temperature fluctuations. The former are in fact propagating sound waves and light scattered, at the appropriate Bragg scattering angle, from such a high-frequency, moving grating of density fluctuations is Doppler shifted from the original frequency. With light scattered from both the oncoming and retreating sound waves the scattered spectrum thus comprises up- and down- shifted light to give the symmetrically placed

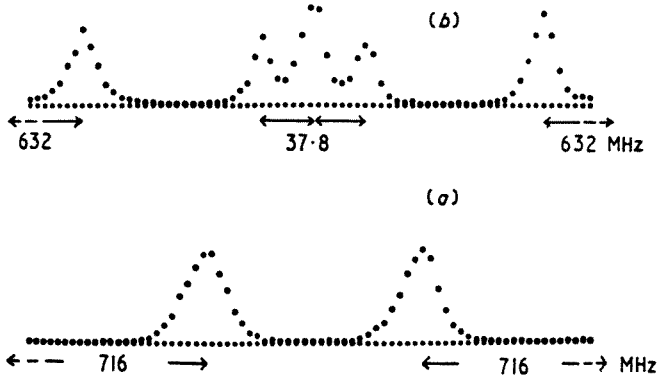

Figure 2. Spectral recordings of light scattered from superfluid helium at 1.25 K. The incident light is at the centre of the picture and there are ∼700 photon counts per channel in the peak of each line. (a) Pure ^{4}He: unshifted scattering is absent and the peaks are from first sound overlapped ∼1.7 orders. Entropy fluctuations, which in an ordinary liquid contribute a central component, propagate as second sound and give little net density change and only weak scattering. (b) A mixture of 43% ^{3}He in ^{4}He. The outer doublet is scattering from first sound; the inner doublet is scattering from second sound (with density fluctuations due to ^{3} He in the normal fluid). The unshifted central component is due to concentration fluctuations [2].

Brillouin doublet around the incident frequency. In contrast the temperature or entropy fluctuations are non-propagating in a normal fluid and decay away diffusely; their scattering contribution, the Rayleigh line, is unshifted at the original laser frequency, with line width determined by the diffusional decay. Thus in the normal state of liquid helium a triplet spectrum—central Rayleigh line and Brillouin doublet—is expected. Below the λ-point, in the superfluid state, this changes and the entropy fluctuations become propagating in the phenomenon of second sound. However for such waves there is a counterflow of normal and superfluid liquid to give a very small net change of density and little scattering. Thus in the superfluid state of pure ^{4}He one expects an ordinary Brillouin doublet from the first sound, the central Rayleigh line to be absent and only a very weak scattering doublet from the second sound.

Just such an experimental spectrum for pure ^{4}He is illustrated in figure 2(a) and followed our first report [1] of experimental observations in 1969. This ^{4}He spectrum presents a remarkable comparison with figure 2(b) showing the light scattering from a mixture of ^{3}He and ^{4}He. In this case the ^{3}He is caught up in the normal fluid component [2] so that in the counterflow of second sound there is now an appreciable density fluctuation and hence light scattering. This is manifest in the Brillouin doublet shown, with frequency shift of ±37.8 MHz corresponding to the much reduced speed of the second sound waves (about 6% of the first sound under these conditions). However in addition there are also non-propagating concentration (hence density) fluctuations of the ^{3}He and ^{4}He and these give rise to the comparatively strong central, unshifted, component also shown in figure 2(b).

For these measurements we were employing plane Fabry–Perot interferometers of up to 100 cm spacing with piezo-electric scanning and recording times of several hours. In later work at RRE Malvern and Birmingham, instrumental line widths of $\lesssim$1.2 MHz were obtained with confocal interferometers of 100 and 150 cm spacing. Several different regimes of liquid helium were explored [3–5]; figure 3 shows spectra in the hydrodynamic region of ^{4}He below the superfluid transition at elevated pressure (20 bar) where the density fluctuations in second sound become appreciable; [6] provides a comprehensive review of this work, and a detailed comparison with theory of the dynamical behaviour of helium near the superfluid transition.

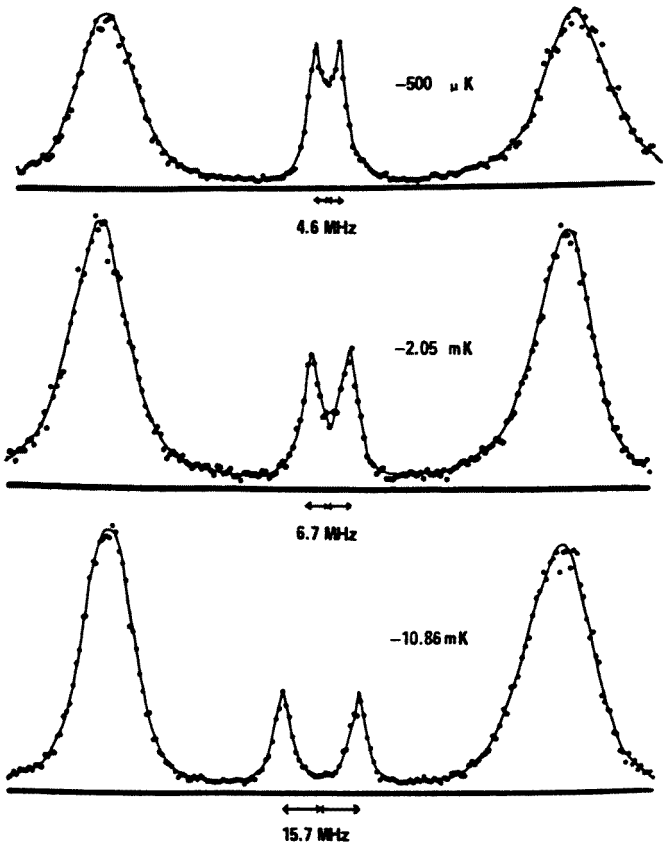

Figure 3. Spectra obtained with a scanning Fabry–Perot interferometer in the hydrodynamic regions of liquid ^{4}He below the superfluid transition and at a pressure of 20 bar [3]. The laser frequency is at the centre of the recording and the outer peaks are due to the first sound overlapping about ± 5.5 orders ($\sim$1000 MHz). The smaller peaks are the second sound doublet.

3. Coherent spectroscopy and helical light beams

The frequency resolution approaching 1 MHz in the later helium work was clearly at the practical limit of that attainable by classical interferometric methods. It thus became obvious to investigate the then rapidly developing field of time-domain spectroscopy for laser scattering (see e.g. [7]). This included photon correlation, intensity fluctuation and coherent heterodyne techniques. Common to all these is the post-detection analysis of the time-varying electrical signal following detection of the light field under investigation. The celebrated Hanbury Brown and Twiss experiments of the 1950s had established the fluctuating character of light fields, with fluctuation times inversely proportional to the frequency band width of the light $\Delta\nu$. Classical spectroscopy had been able to proceed on the basis of 'constant' intensity light sources since the fluctuations for such broad band sources were more rapid than could be followed by the fastest available detectors. However slowly fluctuating light fields, as evident in many beautiful phenomena of laser scattering and speckle, were readily studied with the new time-domain methods.

Comparison of these methods with classical techniques proved very revealing. In the time domain it is essential to isolate a single optical mode (or fraction thereof) of the field

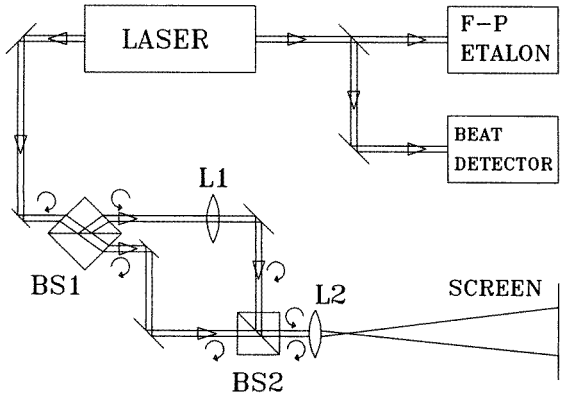

Figure 4. Experimental arrangement. A circular absorber and aperture are inserted into the laser cavity and the laser output monitored on the Fabry–Perot interferometer and beat frequency detector. In the lower interferometric arrangement lens L_1 sets up a difference of curvature in the two beams which are recombined at beam splitter BS2. The helicity of each beam at different points is indicated [13].

under study. This may be done spatially with a simple pinhole aperture or optically by beating it (heterodyning) with the coherent beam of a single mode laser. The resultant strength of signal is then very dependent on the photon degeneracy δ—that is the mean number of photons detected within this single optical mode per fluctuation period $\Delta\nu^{-1}$. For $\delta < 1$ the effective signal becomes very weak; thus for $\Delta\nu \sim 1$ MHz a very high count rate of $\sim 10^6$ photo-detections per second would be required. In great contrast the classical methods operate by direct interferometric filtering or frequency selection of the electromagnetic field (and may be collected across many optical modes), and the separate spectral elements are then detected. Such post-filtering detection can take place over a very long time scale—as in the helium work with a few hundred photon counts collected over several hours. Thus, in principle, classical interferometric spectroscopy can be said to be enormously more sensitive, at least for stationary phenomena in the requisite frequency range which can be examined over a long period.

Nevertheless, time-domain coherent methods have enormous applicability both in the laboratory for all manner of studies of materials, surfaces, light fields and laser physics, etc and also for remote sensing in the outdoors from ground, airborne and potentially space-borne platforms (see e.g. [8, 9]). The present purpose is not to review this enormous field but rather to outline the phenomenon of optical vortices or helices revealed by studies of coherence. In photon correlation studies of the late 1970s various anomalies were found in the amplitude of fluctuations of scattered light using an argon ion laser source of apparently good single mode of lowest order, Gaussian TEM_{00} form. These anomalies were eventually traced to contamination by higher order modes; on examination it became clear that a compound mode TEM^*_{01}, combining two orthogonal TEM_{01} two-spot modes in phase and space quadrature, was in fact a helical mode of hitherto unsuspected form [10].

The surfaces of constant phase (modulo 2π) in a collimated monochromatic beam of light are usually considered to be a series of discs, normal to the beam axis, spaced one wavelength λ apart. However it is perhaps not widely appreciated, even among optical scientists, that monochromatic beams can possess a continuous cophasal surface of helical form extending through space. Such helical waves must of course satisfy Maxwell's equations; not surprisingly the phase discontinuity on axis necessitates a null in the intensity distribution,

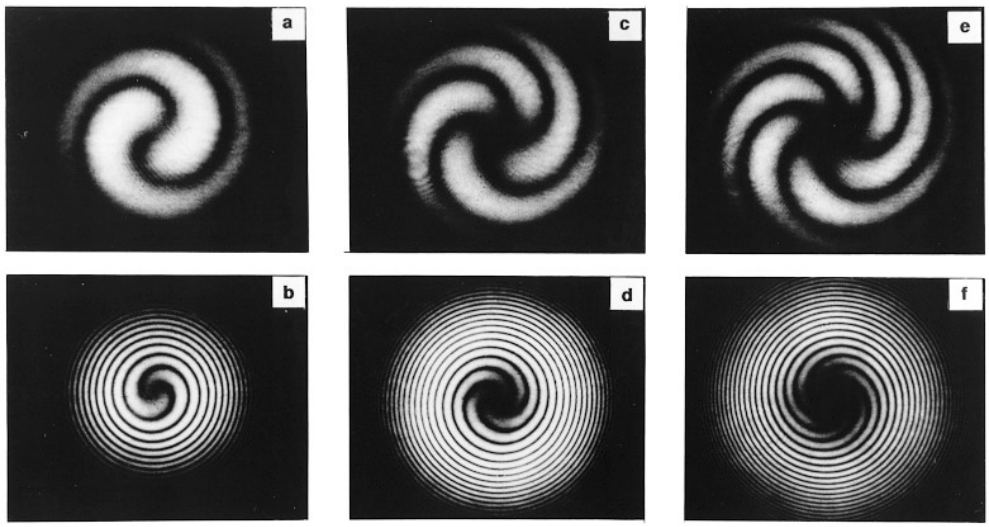

Figure 5. Spiral fringe patterns with the laser operating on doughnut modes of different order: 01* (a), (b); 02* (c), (d) and 03* (e), (f). The beam curvature difference for the upper row is small (less than one wavelength) and for the lower row it is several wavelengths. Note the multi-start spirals (two, four and six respectively) and also the differing handedness of (b) and (f) (clockwise) from which the absolute helical sense can be established [13].

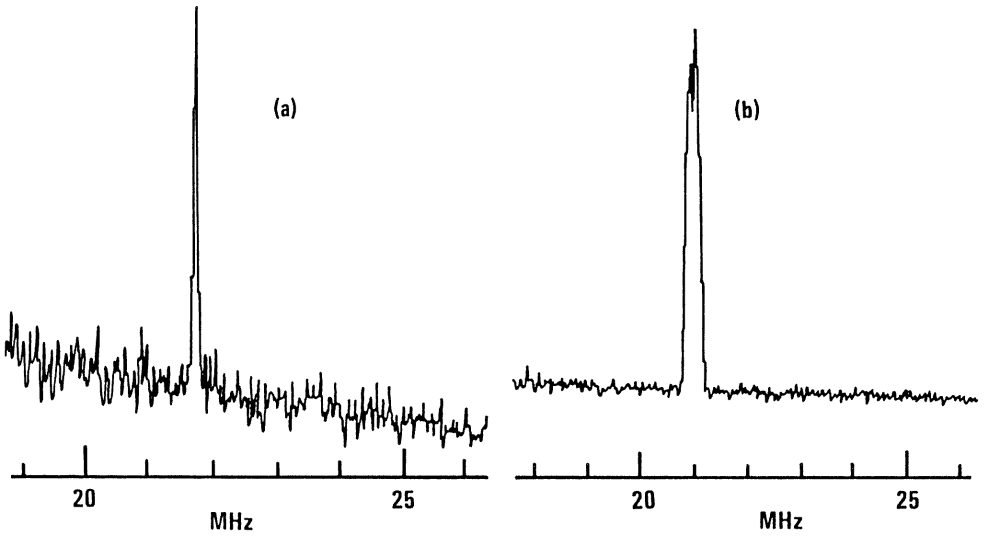

Figure 6. Doppler spectra in the atmosphere recorded with an airborne lidar at focal range of 100 m and in a period of 25 ms; (a) height 5000 ft, peak frequency corresponds to 225.2 knots true airspeed, (b) height 960 ft, mean frequency corresponds to 215.0 knots, note the increased width due to turbulence of ∼5 knots [14].

as apparent in so-called laser 'doughnut' modes. The concept of screw and edge dislocations in wave fronts was first introduced by Nye and Berry [11] in 1974 originating in attempts to understand radio echoes from the bottom of Antarctic ice sheets; analogous experiments were carried out in the laboratory using ultrasound. In our first demonstrations at optical

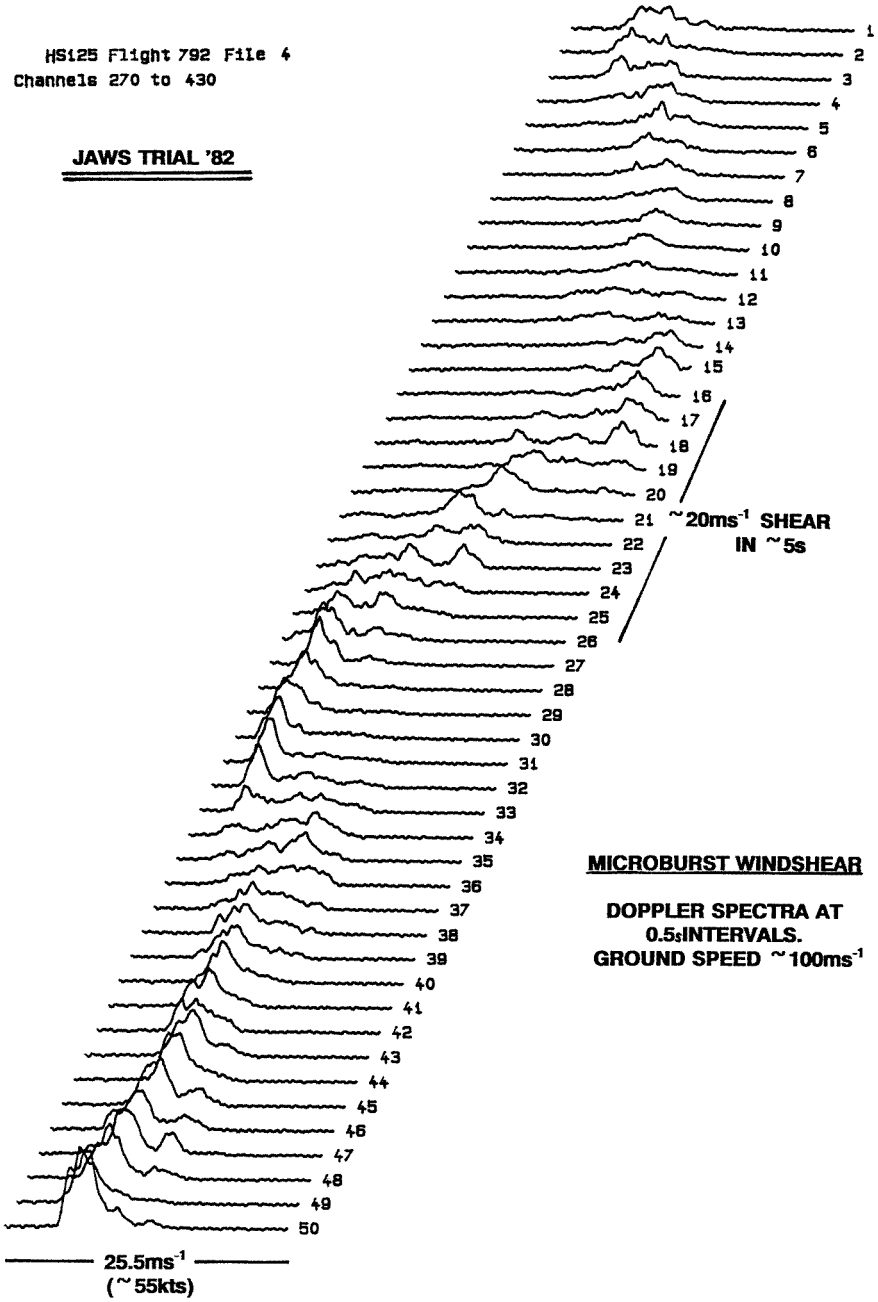

Figure 7. Sequence of lidar spectra recorded at 0.5 s intervals by an airborne lidar during passage through a thunderstorm microburst. Note the wind shear of $\sim$20 ms^{-1} in 5 seconds on passage into the core of the microburst [14].

frequencies, the helices in the lowest order doughnut mode of an argon ion laser were shown to be evolving between left- and right-hand helicity, at the frequency difference of the two constituent TEM_{01} modes [10]. The impact of such spatial coherence properties on various

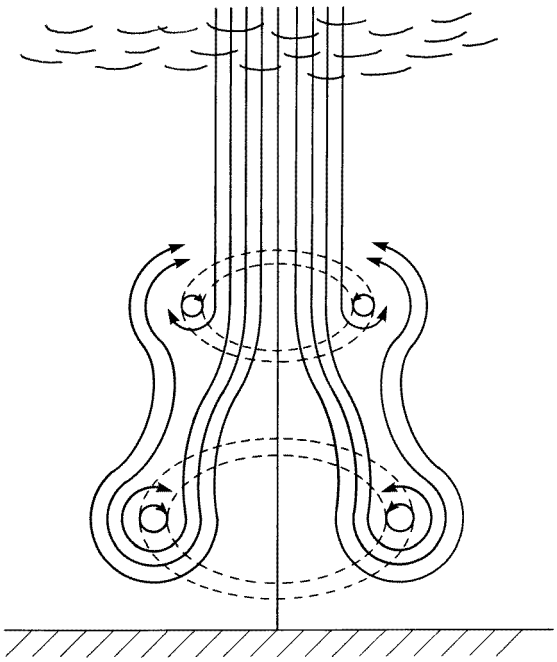

Figure 8. Ring vortex model of a microburst showing streamlines developed from lidar measurements.

laser applications, including photon correlation spectroscopy, fringe velocimetry, speckle and coherent processing was also studied [12]. More recently it has been possible to generate pure, higher order, helical modes [13] of single frequency, and to demonstrate these very clearly with the equipment shown in figure 4. The aim of this arrangement is threefold: after splitting at beam splitter BS1 the two equal beams are recombined at BS2 with (a) different curvature, (b) reversed handedness (i.e. helicity) and (c) equal size at the screen. Variations of curvature are achieved with a selection of lenses L_1 of different focal length whose precise position is adjusted to achieve condition (c) above. The overall change of handedness arising from the different reflections at beamsplitters and mirrors is indicated in figure 4. It must be emphasized that this refers to the helicity of the beams; they remain linearly polarized throughout. As shown the two beams arrive with opposite helicity at the screen; figure 5 shows the spiral fringes that result from this, directly manifesting the helical character of the component beams.

The sets of fringes in figure 5 have been selected to demonstrate the effect of varying curvature difference for 01* and the higher order 02* and 03* modes. In the upper row the small curvature difference amounts to less than one wavelength across the beams; only a fraction of a spiral extends across the beam front. The four-start and six-start spirals for the higher order modes are strikingly evident in each pair of photographs. Such multistart cophasal surfaces obviously require that the pitch of each individual helix much be $m\lambda$ with $m = 1, 2, 3, \ldots$ and λ the wavelength. Figure 5 illustrates the helical character of a carefully prepared laser field. However, on examination, such optical vortices in fact are widespread throughout laser speckle patterns where 2π discontinuities of phase often occur at nulls of intensity (see [14] for further discussion).

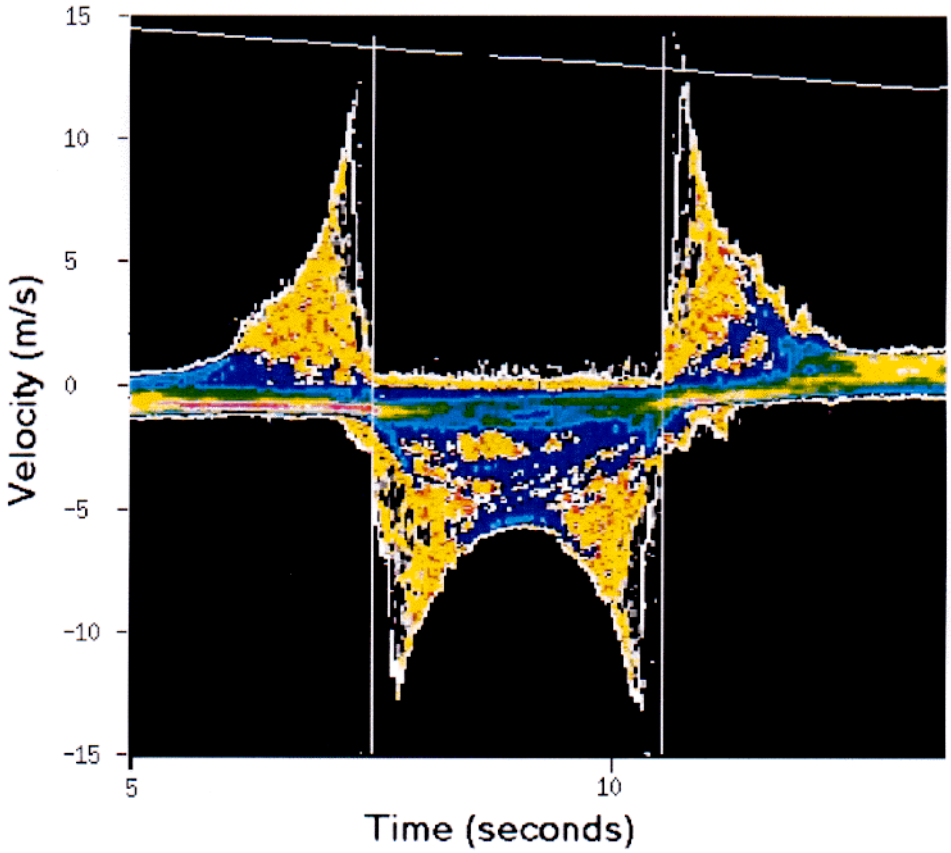

Figure 9. Doppler spectra (recorded at 33 s^{-1}) from a pair of wake vortices generated by an Airbus Industrie aircraft at Toulouse Blagnac airport in March 1998. Each spectrum is plotted vertically and colour coded for amplitude. The time after passage of the aircraft overhead is shown on the horizontal scale and the Doppler velocity component on the vertical scale. The laser beam was scanned in a vertical plane to intersect the vortices; the outline shown in the figure traces out the tangent velocity. The rapidly rising velocity near the core of each vortex (marked by the vertical white lines) is very evident at the sharp change from an upflow to down draught.

4. Large scale vortices in the atmosphere

Doppler measurement of wind velocity and air movement has been one of many applications of laser scattering to practical problems. Coherent heterodyne systems (often known as 'laser radar' or 'lidar'), in which the optical local oscillator beam may be used to dominate the thermal noise of longer wavelength detectors, are particularly effective; in the atmosphere the sources of scattering are small naturally occurring particles, usually referred to as 'aerosols'. Just such a system for airborne operation was built at Malvern in the early 1980s and used widely in studies of true airspeed, wind shear and turbulence, and aerosol scattering high in the atmosphere [15]. Typical Doppler spectra are shown in figure 6 and a sequence of spectra in passage through a thunderstorm microburst in figure 7. These clearly shows the rapidly changing conditions ahead of the aircraft—which are potentially quite dangerous, particularly in the landing and take-off phase. Previous models of such dangerous wind shear from thunderstorm microbursts had been based on simple outflow from a central, falling column of air. Analysis of downburst

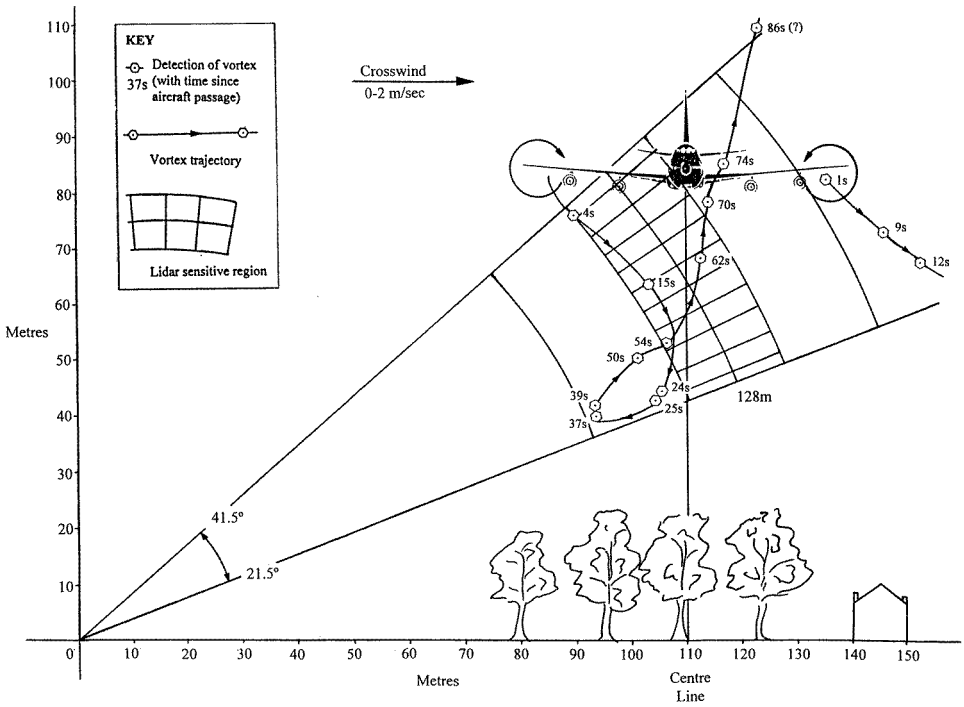

Figure 10. Reconstruction of vortex trajectories from a sequence of records such as figure 9. The lidar was sited ∼110 m north of the centre line with the aircraft (B747-200) about 85 m above ground flying E to W. The lidar was set to focus at ∼128 m range and the scan in the N–S plane is shown as extending over $31.5 \pm 10°$. The light variable cross wind was 0–2 m s^{-1}. The near wing vortex initially descended and then remained stalled at ∼40–50 m for about 30 seconds before rising, with undiminished strength, back to the glide slope at ∼70 seconds.

spectra such as figure 7 showed that the phenomenon was better described by a series of descending ring vortices as illustrated in figure 8. This model is now incorporated in flight simulators for pilot training.

Another potential hazard in aviation is the powerful wake vortices generated by aircraft themselves. In the process of generating lift all aircraft create transverse rotational flow in the air that has passed over each wing. This rotational flow rapidly evolves into two powerful, counter-rotating, vortices that extend as a pair of trailing ribbons behind the aircraft. The characteristics of these wake vortices—their formation, strength, evolution, persistence, trajectory, mode of decay etc—have been studied for many years [16]. The initial separation of the vortices is typically about 80% of the wing span; their rotational sense produces a strong downdraft in the region between them, and in free air they tend to sink at a rate of 1–2 m s^{-1}. The trajectory of the pair of vortices is of course largely determined by the prevailing meteorological conditions; on approach to the ground the sink rate is reduced and the vortices tend to separate. The existence of such vortices represents a potential hazard to following aircraft, particularly for smaller aircraft behind larger. Many studies in the 1970s including laser measurements, helped to define separation minima between various categories of aircraft arriving at and departing from airports. Such separation minima limit the capacity for the world's busier airports; in consequence in the last few years there has been increased interest in the problem of wake vortices.

Figure 9 shows a sequence of Doppler spectra recorded with a lidar beam scanning overhead to intersect a pair of vortices. The high frequency peak of each spectrum gives the tangent velocity of the air flow in the vortex [17]. Thus a sequence of spectra, scanned through the vortices from below, trace out the velocity profile clearly illustrated as the outline in figure 9. Analysis of such data can of course provide information on the structure, transport and decay of full scale wake vortices as they interact with atmosphere. Lidar measurements are thus complementary to computer fluid dynamics modelling, and to reduced scale measurements in wind tunnels. By successive scanning through the vortex field a succession of vortex signatures corresponding to figure 9 is obtained and the vortex trajectories may also be deduced. Figure 10 shows a remarkable (and fortunately very rare) case recorded at Heathrow [18] in which a vortex, after initial descent to ∼40 m, returned close to the aircraft glideslope at ∼85 m altitude, over 60 seconds after passage of the generating aircraft. Analysis shows that the vortex had undiminished strength at this stage but in the next 15 seconds weakened rapidly in the core.

5. Conclusions

Starting from submillimetric quantized vortices in liquid helium, a light scattering path has been traced through optical vortices extending over a few centimetres to aircraft wake vortices of many tens of metres size, and finally descending ring vortices in the atmosphere up to a kilometre in diameter.

Acknowledgments

I am grateful to Dr Mike Harris for help with certain figures. To Joe Vinen I express my deep appreciation of his scientific encouragement and stimulation over many years, and to Joe and his wife Susan my heartfelt, everlasting thanks for their friendship and support.

References

[1] Pike E R, Vaughan J M and Vinen W F 1969 Brillouin scattering from first and second sound in a superfluid ^{3}He–^{4}He mixture *Phys. Lett.* A **30** 373–4
[2] Palin C J, Vinen W F, Pike E R and Vaughan J M 1971 Rayleigh and Brillouin scattering from superfluid ^{3}He–^{4}He mixtures *J. Phys. C: Solid State Phys.* **4** L225–8
[3] Vaughan J M, Vinen W F and Palin C J 1972 Experiments on the scattering of light by liquid helium *Low Temperature Physics-LT 13* vol 1, ed K T Timmerhaus, W J O'Sullivan and E F Hammel (New York: Plenum) pp 532–6
[4] Palin C J, Vinen W F and Vaughan J M 1972 The scattering of light by liquid helium close to the λ line *J. Phys. C: Solid State Phys.* **5** L 139–142
[5] Vinen W F and Vaughan J M 1970 The scattering of light from liquid helium *J. Physique Coll.* **31** C3 29–38
[6] Vinen W F and Hurd D L 1978 Light scattering studies of the dynamical behaviour of liquid ^{4}He close to the λ line *Adv. Phys.* **27** 533–608
[7] Cummins H Z and Pike E R (eds) 1973 Photon Correlation and Light Beating Spectroscopy (New York: Plenum)
[8] Vaughan J M (ed) November 1994 *J. Mod. Opt.* **41** 2063–2196 (separate section of nine papers devoted to coherent laser radar)
[9] Jelalian A V (ed) February 1996 *Proc. IEEE* **84** 99–320 (special issue of eight papers devoted to laser radar)
[10] Vaughan J M and Willetts D V 1979 Interference properties of a light beam having a helical wave surface *Opt. Commun.* **30** 263–7
[11] Nye J F and Berry M V 1974 Dislocations in wave trains *Proc. R. Soc.* A **336** 165–90
[12] Pusey P N, Vaughan J M and Willetts D V 1983 Spatial incoherence of the laser in photon correlation spectroscopy *J. Opt. Soc. Am.* **73** 1012–17

[13] Harris M, Hill C A and Vaughan J M 1994 Optical helices and spiral interference fringes *Opt. Commun.* **106** 161–6

[14] Harris M 1995 Light-field fluctuations in space and time *Contemp. Phys.* **3** 215–33

[15] Woodfield A and Vaughan J M 1983 Airspeed and windshear measurements with an airborne CW CO_2 laser *Int. J. Aviation Safety* **1** 207–24

[16] See e.g. Hallock J N 1991 Aircraft wake vortices, an assessment of the current situation *Report* DOT-FAA-RD-90-29

An annotated bibliography (1923–1990) *Report* DOT-FAA-FD-90-30 (available through National Technical Information Service, Springfield VA 22161, USA)

[17] Constant G D J, Foord R, Forrester P A and Vaughan J M 1994 Coherent laser radar and the problem of aircraft wake vortices *J. Mod. Opt.* **41** 2153–74

[18] Greenwood J S and Vaughan J M Measurements of aircraft wake vortices at Heathrow by laser Doppler velocimetry *Air Traffic Control Q.* **6** 179–203